

REPORT DOCUMENTATION PAGE

*Form Approved
OMB No. 0704-0188*

The public reporting burden for this collection of information is estimated to average 1 hour per response, including the time for reviewing instructions, searching existing data sources, gathering and maintaining the data needed, and completing and reviewing the collection of information. Send comments regarding this burden estimate or any other aspect of this collection of information, including suggestions for reducing the burden, to Department of Defense, Washington Headquarters Services, Directorate for Information Operations and Reports (0704-0188), 1215 Jefferson Davis Highway, Suite 1204, Arlington, VA 22202-4302. Respondents should be aware that notwithstanding any other provision of law, no person shall be subject to any penalty for failing to comply with a collection of information if it does not display a currently valid OMB control number.

PLEASE DO NOT RETURN YOUR FORM TO THE ABOVE ADDRESS.

1. REPORT DATE (DD-MM-YYYY)		2. REPORT TYPE		3. DATES COVERED (From - To)	
4. TITLE AND SUBTITLE				5a. CONTRACT NUMBER	
				5b. GRANT NUMBER	
				5c. PROGRAM ELEMENT NUMBER	
6. AUTHOR(S)				5d. PROJECT NUMBER	
				5e. TASK NUMBER	
				5f. WORK UNIT NUMBER	
7. PERFORMING ORGANIZATION NAME(S) AND ADDRESS(ES)				8. PERFORMING ORGANIZATION REPORT NUMBER	
9. SPONSORING/MONITORING AGENCY NAME(S) AND ADDRESS(ES)				10. SPONSOR/MONITOR'S ACRONYM(S)	
				11. SPONSOR/MONITOR'S REPORT NUMBER(S)	
12. DISTRIBUTION/AVAILABILITY STATEMENT					
13. SUPPLEMENTARY NOTES					
14. ABSTRACT					
15. SUBJECT TERMS					
16. SECURITY CLASSIFICATION OF:			17. LIMITATION OF ABSTRACT	18. NUMBER OF PAGES	19a. NAME OF RESPONSIBLE PERSON
a. REPORT	b. ABSTRACT	c. THIS PAGE			19b. TELEPHONE NUMBER (Include area code)

Sweat rate prediction equations for outdoor exercise with transient solar radiation

Richard R. Gonzalez,¹ Samuel N. Cheuvront,² Brett R. Ely,² Daniel S. Moran,^{3,4} Amir Hadid,³ Thomas L. Endrusick,² and Michael N. Sawka²

¹Biology Department, New Mexico State University, Las Cruces, New Mexico; ²U.S. Army Research Institute of Environmental Medicine, Natick, Massachusetts; and ³Heller Institute of Medical Research, Sheba Medical Center, Tel Hashomer; ⁴Ariel University Center of Samaria, Israel

Submitted 22 August 2011; accepted in final form 9 January 2012

Gonzalez RR, Cheuvront SN, Ely BR, Moran DS, Hadid A, Endrusick TL, Sawka MN. Sweat rate prediction equations for outdoor exercise with transient solar radiation. *J Appl Physiol* 112: 1300–1310, 2012. First published January 12, 2012; doi:10.1152/jappphysiol.01056.2011.—We investigated the validity of employing a fuzzy piecewise prediction equation (PW) [Gonzalez et al. *J Appl Physiol* 107: 379–388, 2009] defined by sweat rate (m_{sw} , $g \cdot m^{-2} \cdot h^{-1}$) = $147 + 1.527 \cdot (E_{req}) - 0.87 \cdot (E_{max})$, which integrates evaporation required (E_{req}) and the maximum evaporative capacity of the environment (E_{max}). Heat exchange and physiological responses were determined throughout the trials. Environmental conditions were ambient temperature (T_a) = 16–26°C, relative humidity (RH) = 51–55%, and wind speed (V) = 0.5–1.5 m/s. Volunteers wore military fatigues [clothing evaporative potential ($i_{m/clo}$) = 0.33] and carried loads (15–31 kg) while marching 14–37 km over variable terrains either at night ($N = 77$, trials 1–5) or night with increasing daylight ($N = 33$, trials 6 and 7). PW was modified ($\dot{P}_{w,sol}$) for transient solar radiation (R_{sol} , W) determined from measured solar loads and verified in trials 6 and 7. PW provided a valid m_{sw} prediction during night trials (1–5) matching previous laboratory values and verified by bootstrap correlation (r_{bs} of 0.81, $SE \pm 0.014$, $SEE = \pm 69.2 g \cdot m^{-2} \cdot h^{-1}$). For trials 6 and 7, E_{req} and E_{max} components included R_{sol} applying a modified equation $\dot{P}_{w,sol}$, in which $m_{sw} = 147 + 1.527 \cdot (E_{req,sol}) - 0.87 \cdot (E_{max})$. Linear prediction of $m_{sw} = 0.72 \cdot \dot{P}_{w,sol} + 135$ ($N = 33$) was validated ($R^2 = 0.92$; $SEE = \pm 33.8 g \cdot m^{-2} \cdot h^{-1}$) with PW β -coefficients unaltered during field marches between 16°C and 26°C T_a for $m_{sw} \leq 700 g \cdot m^{-2} \cdot h^{-1}$. PW was additionally derived for cool laboratory/night conditions ($T_a < 20^\circ C$) in which E_{req} is low but E_{max} is high, as: PW_{cool} ($g \cdot m^{-2} \cdot h^{-1}$) = $350 + 1.527 \cdot E_{req} - 0.87 \cdot E_{max}$. These sweat prediction equations allow valid tools for civilian, sports, and military medicine communities to predict water needs during a variety of heat stress/exercise conditions.

thermoregulation; modeling; load carriage; environmental indexes; fluid replacement

NUMEROUS public health (21, 38), military medicine (6–11, 23, 28, 29) and sports medicine (29, 39) situations exist where it is important to estimate water needs. When performing physical exercise in warm-hot environments, sweat loss is the “critical” factor to calculate water requirements (18, 21, 23, 38). We recently developed from laboratory experiments a fuzzy piecewise equation (PW) that predicts measured sweat losses within a standard error estimate (SEE) of ± 137 ml/h (17). The equation was also validated against several laboratory (indoor) studies with soldiers wearing military clothing-equipment, as

well as one field study (outdoors) in which soldiers wore chemical protective clothing while exposed to constant and low solar loads and low-intensity and high-intensity metabolic rates (M , W/m^2). Therefore, both the initial model development and the validation studies represented conditions impacted by constant mild-to-moderate solar radiation.

Sweating rate (m_{sw} , $g \cdot m^{-2} \cdot h^{-1}$) is calculated from PW as: $147 + 1.527 \cdot (E_{req}) - 0.87 \cdot (E_{max})$ (17). Prediction accuracy is improved by 50–60% over legacy equations (41) and PW has wide applicability to a broader range of environmental temperatures, metabolic rates, and modern military clothing equipment configurations. However, it is unknown if the PW equation provides an improvement over other conventional equations that predict sweat loss with solar load (42). Furthermore, PW has not been validated over extensive military operational missions (outdoors) that encompass heat loads from transient solar radiation. Previous studies have shown that sweat rate is altered by solar heat flux (14, 30) and the whole body sweat rate is elevated proportional to the magnitude of thermal and exercise load. Accurate measurements of required evaporative heat loss (E_{req}) can be predicted by analyzing key heat exchange parameters of the heat balance equation (5, 15, 20, 24). The impact of solar radiation in modifying heat exchange, and thus sweat rate prediction, is easily determined empirically (15, 16, 24, 25, 30). The most strenuous military operations are often conducted in early morning hours that are subject to transient solar radiation coupled with cooler environmental temperatures. A requirement exists to carefully measure sweat rate during outdoor military activities with and without solar radiation to determine the validity of the PW equation for these conditions and ascertain if PW should be modified from appropriate empirical measurements.

The purposes of this study were 1) to validate the original PW sweat prediction equation, derived from laboratory studies, for implementation outdoors at night and with transient solar circumstances in soldiers performing military activities and wearing military clothing-equipment; and 2) to decide whether a modified PW equation should be developed de novo, and if so, then determine if it provides a reliable prediction of sweat rate during prolonged work with transient solar radiation conditions. Our hypothesis was that regression coefficients in the fuzzy piecewise algorithm deriving the PW (15, 44) would be robust enough to permit valid m_{sw} predictions during outdoor night marches, but would require adjustment ($\dot{P}_{w,sol}$) for transient solar radiation exposures and possibly cooler conditions. Consequently, an additional hypothesis was that the PW equation, adapted with required solar load factors, will provide a reliable sweat loss (water needs) prediction equation that is

Address for reprint requests and other correspondence: S. N. Cheuvront, U.S. Army Research Institute of Environmental Medicine, Kansas St., Bldg. 42, Natick, MA 01760 (e-mail: samuel.n.cheuvront@us.army.mil).

Table 1. Description of conditions for the night marches (trials 1–5)

Trial	N	Section	Time, min	Distance, km	Terrain Type, % of Section	Terrain Factor (η)
1 and 2	25	1	60	6	Base course, 40%; sand, 60%	1.4
		2	50	5	Hard road, 40%; plowed field, 10%; hard road, 50%	1.4
		3	50	5	Hard road, 40%; plowed field, 10%; hard road, 50%	1.4
		4	68	5	Base course, 40%; sand, 60%	1.4
		5	30	3	Base course, 40%; sand, 60%	1.4
3	12	1	60	6	Hard road, 40%; wet hard sand, 60%	1.5
		2	50	5	Hard road, 40%; plowed field, 10%; hard road, 50%	1.5
		3	65	6.5	Wet hard sand, 80%; dry sand, 20%	1.5
		4	65	6.5	As above	1.5
		5	55	5.5	Same as section 2	1.5
		6	75	7.5	Dry sand, 80%; 1 km on hard road, 20%	1.5
4 and 5	40	1	55	6	Trial 4: -7.3 km/h (%gradient -0.7) descent on gravel, 15 min rest; trial 5: -9.6 km/h (%gradient -0.8), 15 rest	1.3
		2	55	6	Trial 4: 10 km/h ascent on gravel; 17 min rest; trial 5: 7.8 km/h (% gradient 0.7) ascent; 17 min rest.	1.3
		3	28	2	Trial 4: -16.1 km/h (%gradient -0.8) descent on gravel, completion; trial 5: 1.7 km/h ascent (%gradient 0.2), march completion.	1.3

N is number of volunteers completing each trial. Section is the type of road during each march, % time, and various ascent/descent (km/h; %gradient) marches of trials 4 and 5. Terrain factor (η) is unit coefficient of Pandolf equation prediction (31, 32), as modified by Santee et al. (35) for specific descent marches.

functional for a wide range of indoor and outdoor operational scenarios with improved prediction over legacy equations (41, 42) and other modeling approaches (3, 24, 46) that account for solar radiation. As in the previous study (17), we applied Tseng's and coworkers (44) fuzzy piecewise analysis to predict sweat losses measured from field data assuming that m_{sw} (lumped efferent eccrine output) has both linear and nonlinear characteristics as a function of core temperature (T_{core}) and skin temperature (T_{sk}) inputs (15, 24, 37). Nonthermal factors (43) that may affect the general gain of the efferent thermal drive and sweating threshold were not accounted for in the analysis. The sweat loss equations (indoor and transient solar load) in the present study should be considered as lumped derivatives and include central nervous system sudomotor drive principally from thermal factors with nonthermal factors having minimal effect (37).

METHODS

One-hundred ten male soldier volunteers participated in numerous outdoor field trials. The appropriate institutional human use review boards approved the protocol, and all volunteers provided written informed consent. Investigators adhered to policies for protection of human subjects as prescribed in US Army Regulations 70–25 and US Army Medical Research and Materiel Command Regulation 70–25. The research was conducted in adherence with the provisions of Code 45 of Federal Regulation part 46.

Experimental studies. Experimental data were collected by staff of the Heller Institute of Medical Research. Seven outdoor marches were performed by active military units and incorporated into their training,

with accommodations made for careful data collection. The military units maintained normal leadership, training hours, clothing-equipment, and work rates (load and speed) applicable to actual missions. Exercise level per se, state of hydration, and sleep state in the subjects all were controlled. Subjects were well-hydrated at the beginning and during rest, and none of the subjects was sleep deprived.

The outdoor marches were conducted near field stations exhibiting diverse terrains (desert, Mediterranean coastal, and various foothill areas). Tables 1 and 2 describe the number of subjects and specific conditions for the night (trials 1–5) and transient solar radiation (trials 6 and 7) outdoor marches, respectively. Data were collected on 77 volunteers who marched at night (trials 1–5), and some of these individuals participated in multiple trials. Thirty three supplementary volunteers marched during the transient solar radiation conditions (trials 6 and 7). Table 3 shows many of the variables and equations with essential modifications used in the study.

Physiological measures. Oxygen uptake was measured from a cohort of the volunteers. These data were then used to estimate metabolic rate of other individuals in each group. Metabolic rate was calculated from a 90-s sample of expired air collected using a K4B (COSMED, Italy) metabolic measurement device. Marching pace and grade were estimated using a Garmin GPS navigator. Oxygen uptake calculations were estimated based on weight, load, walking speed + grade, and terrain factor using Pandolf et al. (32) equations and Santee et al. (35) modifications for some downhill trials to estimate net heat production. In some cases, a median terrain factor coefficient was chosen since portions of some marches occurred on gravel, sand, and paved road (Tables 1 and 2). The oxygen uptake calculation was for the exercise portion only, as rest periods were estimated at a metabolic rate of 120 W (average of 63 ± 3 W/m²) (15, 24). A standard respiratory exchange ratio for a mixed diet was estimated for consis-

Table 2. Description of conditions for the transient solar load marches (trials 6 and 7)

Trial	N	Section	Time, min	Distance, km	Terrain Type/% of Section	Terrain Factor (η)
6	20	1	65	6.0	Gravel, 100%; 18-min rest period	1.30
		2	48	4.4	Gravel, 100%; 17-min rest period	1.30
		3	62	6.0	Gravel, 100%	1.30
7	13	1	58	5.8	Paved road, 43%; gravel, 57%	1.25
		2	71	6.7	Gravel, 100%	1.25
		3	62	5.8	Paved road, 43%; gravel, 57%	1.25

Abbreviations are same as Table 1. Trial 6 began at 0330 and ended at 0700; average global solar load (gSL) monitored from 2 stations = 63 W/m². Trial 7 began at 1420 and ended at 1800; average gSL = 265 W/m².

Table 3. Nomenclature and description of key variables and equations implemented

Variable	Units	Description	Formula	Refs.	Modification in Present Study
PW	$\text{g} \cdot \text{m}^{-2} \cdot \text{h}^{-1}$	Sweat rate prediction by fuzzy piecewise (PW) change point regression	$147 + (1.527 \cdot E_{\text{req}}) - (0.87 \cdot E_{\text{max}})$	17, 44	Calculation by bootstrap correlation of original and night field data: equation remains valid $N > 500$ cases; outliers do not statistically change comparison; SEE within $\pm 69 \text{ g} \cdot \text{m}^{-2} \cdot \text{h}^{-1}$
M	W/m^2	Metabolic heat production	Calculated from measured oxygen uptake ($\dot{V}\text{O}_2$) and Pandolf equation	15, 32, 35	Pandolf equation adjusted by Santee coefficients
$\dot{P}_{\text{w},\text{sol}}$	$\text{g} \cdot \text{m}^{-2} \cdot \text{h}^{-1}$	Sweat rate prediction for transient solar load	$147 + (1.527 \cdot E_{\text{req},\text{sol}}) - (0.87 \cdot E_{\text{max}})$	This study, Fig. 3	Solved for R_{sol} per march time using transient solar field data; sweat rate becomes predictable as OLS equation: $0.72 \cdot \dot{P}_{\text{w},\text{sol}} + 135$, $R^2 = 0.92$
E_{max}	$\text{g} \cdot \text{m}^{-2} \cdot \text{h}^{-1}$	Maximum evaporation capacity of a given environment	$E_{\text{max}} = \omega h_c (P_{\text{s},\text{sk}} - P_{\text{a}})$	15	Adjusted by skin wettedness (ω). The fraction of the total body area (A_{D}) covered by sweat [wetted area (A_{w})], i.e., $A_{\text{w}}/A_{\text{D}}$, and evaporative heat transfer coefficient, h_c
E_{req}	$\text{g} \cdot \text{m}^{-2} \cdot \text{h}^{-1}$	Required evaporation from heat balance includes total skin evaporation, all respired, non eccrine, and metabolic water losses	$E_{\text{req}} = M - (\text{Wext}) - \text{DRY} - S$	15	Valid for indoor lab and night field data; for transient solar field study, $E_{\text{req},\text{sol}}$ first solved for R_{sol} as input to heat balance equation to determine $\dot{P}_{\text{w},\text{sol}}$.
$R + C$	W/m^2	Dry or sensible heat loss	$[6.45 \cdot (T_{\text{a}} - T_{\text{sk}})]/I_{\text{T}}$	4, 15	Modified by ambient temperature and water vapor pressure, maximum T_{a} and P_{a} , evaporative potential (E_{max}), respiratory exchange ratio (R)
E_{res}	W/m^2	Respiratory heat loss	$(E_{\text{res}} + C_{\text{res}}) = A_{\text{d}} \cdot M [0.0014$	15	
C_{res}	W/m^2	Convective heat loss	$(34 - T_{\text{a}}) + 0.0023 \cdot (44 - P_{\text{a}})]$		
E_{dif}	W/m^2	Skin diffusion	$E_{\text{dif}} = 0.05 \cdot E_{\text{max}}$	15	
m_{res}	g/min	Metabolic heat loss	$m_{\text{res}} = \dot{V}\text{O}_2 \cdot (R \cdot 0.53)$	17	
P_{a}	kPa or Torr	Ambient water vapor pressure	$(\text{RH}/100) \cdot \exp[18.6686 - (4030.183/T_{\text{a}} + 235)]$; Antoine equation	15	
h_c	$\text{W} \cdot \text{m}^{-2} \cdot ^\circ\text{C}^{-1}$	Convective heat transfer coefficient	$h_c = 1.2 \cdot [(M - 50) \cdot (P_{\text{B}}/760)]^{0.39}$	15	Modified by walking, free and forced convection, barometric pressure (P_{B}), Lewis relation at sea level ($2.2^\circ\text{C}/\text{Torr}$)
h_e	$\text{W} \cdot \text{m}^{-2} \cdot ^\circ\text{C}^{-1}$	Evaporative heat transfer coefficient	$2.2 \cdot h_c$ or alternatively, with clothing $(2.2 \cdot i_{\text{m}})/(I_{\text{T}} \cdot 0.155)$		
h_r	$\text{W} \cdot \text{m}^{-2} \cdot ^\circ\text{C}^{-1}$	Radiative heat transfer equation	$h_r = 5.67 \cdot 10^{-8} \cdot 0.97 \cdot 0.77 \cdot [(T_{\text{sk}} + 273)^4 - (\text{MRT} + 273)^4]/(T_{\text{sk}} - \text{MRT})$	15	Unmodified
I_{T}	clo	Total clothing insulation, sum of air (I_{a}) and fabric (I_{cl}) layer insulation	$(I_{\text{a}} + I_{\text{cl}})$	4, 15	clo = $0.155^\circ\text{C} \cdot \text{m}^2/\text{W}$ or thermal conductance of $6.45 \text{ W} \cdot \text{m}^2/\text{K}$
F_{cle}	ND	Effective clothing factor for heat exchange from articulated manikin			
$P_{\text{s},\text{sk}}$	kPa or Torr	Skin saturation vapor pressure	Antoine equation solved for T_{sk}	15	
R_{cl}	$\text{m}^2 \cdot \text{K}/\text{W}$	Intrinsic (fabric) thermal resistance	$R_{\text{cl}} = R_{\text{T}} - 1/[(h_c + h_r) \cdot f_{\text{cl}}]$	1, 15	Reciprocal of thermal conductance
R_{t}	$\text{m}^2 \cdot \text{K}/\text{W}$	Total clothing resistance	$0.155 \cdot I_{\text{T}}$	1, 15	Modified by wind and body motion
V_{air} or V	m/s	Ambient air movement (velocity on person)	Input variable	7, 15, 17	Direct observations
V_{eff}	m/s	Effective air motion produced by wind speed and M	$v_{\text{air}} + (0.004) \cdot (M \cdot A_{\text{D}} - 105)$	24, 32	Unmodified
σ		Stefan-Boltzman constant	$5.67 \times 10^{-8} \text{ W} \cdot \text{m}^{-2} \cdot \text{K}^{-4}$	1, 15	Unmodified
W_{ext}	W/m^2	External work based on activity	Pandolf equations	32	Santee (35) modifications
A_{P}	m^2	Projected surface area exposed to direct beam solar flux	Fanger, ASHRAE equations	1, 13	Upright walking
f_{eff}	%	Fraction of body surface exposed to solar load at a given time ($A_{\text{P}}/A_{\text{D}}$)	Fanger, ASHRAE equations	1, 13	Upright walking
α_{LW}	W	Long wave absorptivity	Breckenridge and Goldman equations	4, 16	Upright walking
α_{SW}	W	Short wave absorptivity	Breckenridge and Goldman equations	4, 16	Upright walking

Continued

Table 3.—Continued

Variable	Units	Description	Formula	Refs.	Modification in Present Study
R _{sol}	W	Matthew solar radiant heat flow	$-0.0003 \cdot (\text{gSL})^2 + 0.681 \cdot (\text{gSL}) + 3.136$	25	Adjusted by A _D and F _{cl,e} for inclusion into heat balance to determine E _{req, sol} (W/m ²)
ERF	W/m ²	Effective radiant field	$h_r \cdot (\text{MRT} - T_a); @ [(0.835 \cdot R_{\text{sol}})/A_D]$	15	Interchangeable variables
gSL	W/m ²	Global solar load	Direct weather station data; pyranometer values	25	Direct measurement from weather station data
I _{TH}		Total solar irradiance of a horizontal object	$R_D \cdot \sin \beta + R_{\text{dif}}$	2, 13	Meteorological variables
Me,th		Radiant flux emitted as thermal radiation by a surface.	Shapiro et al., outdoor equations	42	Unmodified
MRT	°C	Mean radiant temperature	$T_a + \text{ERF}/h_r$	14, 15	Unmodified
T _{sk}	°C	Mean weighted skin temperature	Mitchell equation	27	3-Site direct measurement
V _{air}					Direct measurement
R _D	W	Direct beam solar load	Arens et al., Breckenridge, and Fanger equations	2, 4, 13,	Direct or weather station values
R _{dif}	W	Diffuse irradiance			
R _{ref}	W	Reflected irradiance			
A _D	m ²	Body surface area (BSA) from DuBois equation	$A_D = 0.202 \cdot W^{0.425} \cdot H^{0.725}$	1, 15	Observed values

tency based on a respiratory exchange ratio during submaximal intensity exercise (50% $\dot{V}O_{2\text{ peak}}$) ranging from 0.8 to 0.98 (7, 13).

Although not reported, heart rate and core temperature were measured for medical monitoring purposes. Heart rate was recorded using a Polar heart rate monitor. Core temperature data were recorded using the telemetric pill technique (HQ and Mini Mitter). During the rest periods, three-site skin temperatures were measured by an YSI-409 (YSI, Yellow Springs, OH) surface thermal probe. Mean weighted skin temperature (\bar{T}_{sk}) was calculated using a three-site (chest, thigh, and arm) surface area weighting coefficient formula (27). In the present data set, clothed \bar{T}_{sk} was linearly correlated with T_a by the equation: $\bar{T}_{\text{sk}} = 0.53 \cdot T_a + 20.28$ ($R^2 = 0.83$; $\text{SEE} = \pm 0.54$) over the range of T_a from 16 to 26°C. Skin saturation vapor pressure (kPa) was determined for each individual skin temperature value using Antoine's equation (15, 24) and the necessary evaporative heat transfer coefficients (h_e) utilized to determine E_{max} for each time interval in the respective trials.

Total sweat losses were determined from changes in body mass, corrected for nonsweat losses, and assume that sweat volume and mass are equivalent (1 ml = 1 g). Sweating rate expressed as liters/h or $\text{g} \cdot \text{m}^{-2} \cdot \text{h}^{-1}$ was determined by time and surface area weightings, as appropriate. Detailed calculations included (7):

$$m_{\text{sw}} = \left[\Delta \text{nude body mass} - (\text{UV} + \text{EW} + \text{NEFL}) + \text{DV} \right] / \text{time} \quad (1)$$

where Δ nude mass is the difference in nude body mass (g) pre- to postexercise; UV is urine volume; EW is excrement weight, if any; NEFL is noneccrine fluid losses, which include respiratory water losses and CO₂-O₂ exchange (7, 36, 37); and DV is consumed drink volume. Body mass was measured while the subject was minimally clothed and fully clothed before and after each march for estimation of trapped sweat.

Environmental parameters. The environmental parameters ambient air temperature (T_a , °C), relative humidity (RH, %) (transformed to ambient water vapor pressure, kPa), and wind velocity (V , m/s) were collected every 30 min using a Kestrel 3000 (Caliber Sales Engineering) and recorded manually for later spreadsheet entry. Composite global solar radiation (gSL, W/m²) was recorded at two field stations in close proximity to the marches. The effective solar load was determined by calculation of R_{sol} and effective radiant field (ERF) and mean radiant temperature (MRT) (15, 16, 24, 25). The procedure employed to determine these coefficients for transient solar load will be described later.

Shapiro et al. (42) originally estimated solar radiation effects via several correction factors annexed to their sweat loss prediction equation from data collected during steady-state exposure to a variety of solar load intensities. These factors were used to estimate required evaporative heat loss (E_{req, SL}) by assessing separate thermal radiative flux factors analyzed from the heat balance equation as:

$$E_{\text{req, SL}} (\text{watts}) = M - W_{\text{ext}} + [H_c + H_r + H_L]. \quad (2)$$

In the above equation (42), M is metabolic heat production (15, 32, 35); W_{ext} is external work rate (32); H_c is convective heat transfer, calculated as $6.45 \cdot A_D (T_a - \bar{T}_{\text{sk}}) / I_T$; A_D is the DuBois body surface area (m²) (15); and I_T (4) is the fixed value of total clothing insulation [originally evaluated by a static manikin that include the air (I_a) and intrinsic clothing layers (I_{cl})]. The radiative heat flux factors comprise H_r (W), which was estimated from radiative heat transfer = $[1.5 \cdot A_D \cdot (\text{SLg}^{0.6}) / I_T]$, where SLg incorporates the shortwave radiative load; and long-wave emission (H_L , W) from the total body to the environment, which was estimated as:

$$H_L = (0.047 \cdot A_D \cdot M_{e, \text{th}}) / I_T \quad (3)$$

where the factor ($M_{e, \text{th}}$) is the radiant heat flux that includes the combined theoretical perfect black-body long wave emission from all body surfaces. $M_{e, \text{th}}$ is equal to σ , the Stefan-Boltzman radiation constant ($5.67 \times 10^{-8} \text{ W} \cdot \text{m}^{-2} \cdot \text{K}^{-4}$) multiplied by T^4 , calculated as the outer surface layer temperature (\bar{T}_{cl})⁴ and transformed into °K (273.15 + °C) (4, 15, 25). Effect of heat storage (S) was not accounted for in the above analysis, and steady-state was assumed for all the heat exchange variables.

Several thermal radiation algorithms were derived in the present study quantifying a more inclusive radiative heat transfer analysis possible for the transient state (1, 2, 4, 16, 25). These analyses were applied for evaluating transient solar load on the individual {i.e., when the global solar radiation [$\text{gSL} \cong (H_r + H_L)$] is not constant}. Solar radiation is generally measured as the sum of the total (direct plus diffuse) radiation falling on a horizontal surface (gSL). In meteorologic terms this is expressed as I_{TH}, which varies with solar elevation (1, 2, 16). In addition, the area of the human body exposed to solar radiation, and therefore the solar energy received by the body, also varies with solar elevation. Generally, gSL [or its sequel, I_{TH}, (2, 4)] can be plotted for a specific solar elevation. A key property is the projected area (A_p) solved as a function of the solar altitude and normally is about 20–25° at the highest solar altitude and drops to around 80–90° (1, 2, 13).

The equivalence between I_{TH} , ERF, and MRT (all inclusive radiative heat transfer algorithms) involves the following assumptions. Radiation (R) and convection (C) in the heat exchange are assumed to be equal in plotting MRT. This heat exchange proportionality occurs because the $(MRT - T_a)$ is directly proportional to ERF (14). In the present study, long-wave radiation characterized by MRT and ERF is treated as uniformly distributed (4π) on the individual during each walking phase (15, 16). There exist no provisions for the directional characteristics of the body's exposed surfaces interacting with non-uniformities in the long-wave radiant field (4). The total body surface area of the assumed person impacted by the solar load is initially estimated by A_D (15). The projected area (A_p) of an individual exposed to direct beam solar load while walking is calculated for our purposes as $A_p/A_D = 0.23$ (1, 2, 4, 13–16).

The effective radiant field (ERF) (1, 14, 15) is one convenient and precise measurement of the net radiant heat flux to or from the human body. ERF incorporates the summed long-wave radiation energy received by the body in a clothed state when surrounding surface temperatures are different from the air temperature. Additionally, the surrounding surface temperature may be expressed by MRT over a 4π radiating area of the body surface (14, 15) particularly with sustained marching or when surface temperatures are higher than extremities or other microclimate spaces surrounding the individual. The ERF on the human body is related to MRT by:

$$ERF = f_{eff} \cdot h_r (MRT - T_a) \quad (4a)$$

in which MRT is easily transformed by

$$MRT = T_a + ERF / (f_{eff} \cdot h_r) \quad (4b)$$

where f_{eff} , calculated as (A_p/A_D) , is the fraction of the body surface exposed to radiation from the environment; h_r includes the radiative heat transfer coefficient; and T_a is the air temperature. Typically, any transient solar load by ERF regardless whether it is direct, diffuse, or from the ground up to the individual (W/m^2) divided by the radiative coefficients ($m^2 \cdot K/W$) increases the effective temperature (ET^*) above the prevailing ambient temperature ($^{\circ}C$) and intensifies the heat stress as MRT rises (15, 16, 25). Gagge and Hardy (14) demonstrated that every interval of this radiative heat flux influences ERF and is linearly correlated with thermoregulatory sweating rate assessed by evaporative heat loss from body weight loss changes.

For both trials 6 and 7, the body surface areas of the 33 walking volunteers, as sunlight first appeared, were generally considered as being exposed to mixed diffuse, reflected, and long-wave radiation in which the $f_{eff} = 0.72$ determined using Fanger's projection factors (13). The area exposed was estimated as $0.72 \cdot A_D = 1.37 m^2$ over a body surface of $1.9 m^2$ for the subjects' averages. A solar elevation (β) of 45° was considered for the walks in this study (1, 2, 13, 16). Diffuse-sky and ground-reflected solar radiation (25) were assumed to be uniformly spread on one-half the exposed portion of each of the volunteer's BSA when clothed as $f_{eff} \cdot 0.95 = 0.684 m^2$ over half of the body surface.

Because ERF incorporates the f_{eff} of the receiving individual, for this study the ERF integrates absorbed energy from long-wave (H_L) and shortwave (H_s) sources originally found in the Shapiro (42) formulation estimated as:

$$ERF \cdot \alpha_{LW} = [0.72 \cdot (0.95/1.9) \cdot (R_{dif} + R_{ref}) + (0.41/1.9) \cdot R_D] \cdot \alpha_{SW} \quad (5a)$$

where, for the walking individual, α_{LW} is long-wave absorptivity, $\cong 0.95$; α_{SW} is short-wave absorptivity, $\cong 0.67$ for (white) skin and military clothing (for this study $I_T = 1.26 clo$); R_D is direct beam solar radiation measured perpendicular to the beam (W/m^2); R_{dif} is diffuse irradiance (W/m^2) of an upward-facing horizontal surface; and R_{ref} is reflected irradiance (W/m^2) of a downward-facing horizontal surface.

Since $R_D \cong gSL$ OR $(I_{TH} - R_{dif})/\sin \beta$, assuming I_{TH} is total solar irradiance of a horizontal surface, Eq. 5a can be rewritten:

$$ERF \cdot 0.95 = [(0.72/2) \cdot (R_D + R_{ref}) + (0.41/1.9 \cdot \sin \beta)] (I_{TH} - R_{dif}) \cdot 0.67 \quad (5b)$$

For the present study, from Fanger's estimates (13), R_{ref} was assumed to be $0.23 \cdot I_{TH}$, which is the mean value of the terrain areas during the walks as solar gain (from a specific station gSL value) accumulates on the individual during the time periods.

In general, the average solar radiation load (as gSL or I_{TH}) from the various stations is not always the best approximation to quantify $E_{req,SL}$ because the lumped quantity assumes steady-state direct radiant load and each subject is generally gaining a different net gSL per time during the walk. In this study, we are interested in whole body sweat response affected by the gSL per each work/rest period.

Solar parameter estimation for transient exposures. Matthew et al. (25) extended the above solar radiation calculation approach by developing an equation that is applicable to the transient solar data of the present study data analysis. The equation can be straightforwardly migrated into various heat strain models (24, 31, 46) that input variables of MRT, ERF, and T_a or a combination of these (15, 16, 24). Extending Matthew's calculations, we developed a continuous function that integrates both H_r and H_L [from the Shapiro (42) outdoor study] and the I_{TH} ($\cong gSL$) concept discussed above to evaluate transient solar heat load that each subject is gaining per time during a march. Our improved solution allowed us to resolve the average "constant" solar radiation variations. R_{sol} (W per person in this case) theoretically represents the best-case alternative correcting variable clothing factors and transient radiant loads by MRT and ERF (4, 15, 16). Additionally, Matthew and colleagues (25) reported that R_{sol} and ERF solutions are tightly correlated ($R^2 = 0.93$) over wide solar domains. Their separate influences can therefore be interchanged. As such, MRT that is proportional to ERF becomes a convenient index as an input into various thermal models can be easily solved from both R_{sol} , ERF, and rationally estimated from mean gSL, assuming the given weather station uses standard meteorological measuring instruments.

In the heat flow form expressed by Matthew et al. (25),

$$R_{sol} \text{ (watts)} = -0.0003 \cdot (gSL)^2 + 0.681 \cdot (gSL) + 3.136 \quad (6)$$

In the polynomial fit ($R^2 = 0.93$) of Eq. 6, MRT ($^{\circ}C$) was derived from measurements using a pyranometer (to measure short-wave radiation fluxes) and pyrgeometer (to measure long-wave radiation fluxes). Normally, the value of the solar load differences ($MRT - T_a$) is the effective heat stress input parameter employed in various thermal models (1, 3, 24). This parameter may be solved in the equation to estimate solar load on the skin surface ($H_{s,sk}$) that is currently implemented in the USARIEM Heat Strain Decision Aid (HSDA) in which $H_{s,sk}$ is computed as a function of various clothing factors (γ_{clo} and $\gamma_i = i_m/clo$) and V_{eff} corrected for walking ["pumping" factors (4) and load carriage variables (3, 17, 24, 31, 32, 46)]. In trials 6 and 7, MRT was calculated by solving for the average R_{sol} and its sequel (ERF) at each marching period and time of day from the gSL collected at the various field stations. The variable I_{TH} will not be considered further.

Either R_{sol} or ERF can be utilized in the heat balance equation (as a rational variable in the heat balance equation) by combining the parameters Shapiro (42) employed to evaluate radiative short-wave (gSL, W) and long-wave ($H_{L,g}$, W) heat stress less radiative long-wave heat loss (H_L , W). Applying partitioned calorimetric analysis (15, 16, 24), the heat balance equation (W/m^2) becomes:

$$\pm S = (M - W_{ext}) - E_{sk} - (R + C) + R_{sol} \quad (7)$$

where S is the rate of heat storage less metabolic heat production (M) minus external work rate (W_{ext}), minus radiative (R) and convective heat loss (C), and $E_{sk} = (E - E_{res} - C_{res} - E_{dif} - m_{res})$. The variable (E) incorporates total sweat loss minus respiratory (E_{res}) and convective heat loss (C_{res}) minus skin diffusion (E_{dif}) less any metabolic heat

loss (m_{res}). The R_{sol} in Eq. 7 is calculated as a radiant flux (per m^2). All avenues of heat exchange and respective heat transfer coefficients can be calculated as in previous studies (15, 16, 24).

The transient equation describing heat exchange between the skin surface and the radiant environment varying with time ($E_{req, sol}$) (Table 3) is therefore estimated by:

$$E_{req, sol} (W/m^2) = \text{net heat flux} - \text{DRY} + \text{effective solar gain} \pm \text{heat storage} \quad (8a)$$

$$E_{req, sol} (W/m^2) = M_{sk} - h_{r+c} \cdot F_{cl,e} (\bar{T}_{sk} - T_a) + [R_{sol} \cdot F_{cl,e}] \pm S \quad (8b)$$

where M_{sk} in Eq. 8b now includes the net heat flux from the interior body to the skin ($M - W_{ext} - E_{res} - C_{res} - m_{res}$). The variable $[F_{cl,e}]$ is the effective clothing factor determined from an articulated, movable manikin in separate analysis (4, 13, 16, 24).

In Eq. 8b, equivalent mathematical substitutions can be used assuming $R_{sol} \cong \text{ERF} = h_r \cdot (A_r/A_D) \cdot (\text{MRT} - T_a)$. The variable, $E_{req, sol}$, therefore, represents the solution of all avenues of the heat balance during transient solar loads over a given time interval. The value is substituted into the PW equation and iterated into the fuzzy piecewise analysis (44). An independent computer-generated sensitivity analysis showed that ERF (W/m^2) is thermally equivalent to 0.23 · gSL for each time period of the walks where the gSL is the solar load (W/m^2) as generally reported in the weather field stations. Therefore, the net solar load on the individual is optimally expressed by either R_{sol} or ERF (W/m^2), and both functions can be quantified during transients in algebraically different, but equivalent heat transfer methods, as described below.

During field operations, R_{sol} (W/m^2) can be calculated from $0.835 \cdot \text{ERF}$. If R_{sol} (in W/m^2) is known by direct pyranometer measurements, MRT ($^{\circ}C$) can be estimated from $0.0965 \cdot (R_{sol} \cdot A_D) + T_a$ or vice versa if the MRT is recorded from a black or khaki-colored 6-in. (15.2 cm) globe or 4π radiometer (15, 16, 25). When rough-estimated weather station gSL (W/m^2) values are the only available sources, ERF can be predicted from 0.23 · gSL, and MRT can be determined from the calculated ERF as:

$$\text{MRT} (^{\circ}C) = T_a + \text{ERF} / (f_{cl,e} \cdot h_r) \quad (9)$$

Equation 9 therefore sums the effect of mixed solar radiation from direct, diffused, and ground radiant loads during a given transient solar radiation. The equation can also be used to integrate radiant exchange with the body surface when MRT differs with T_a and estimate the effect of heat storage (S) as the individual exercises over a given period of time throughout variable solar radiation intensities (15).

Heat transfer analyses. In the present study, clothing heat and evaporative potential parameters were determined using a regionally heated, articulated manikin at various wind speeds. Each element of the comprehensive heat balance equation was analyzed from the raw data, specific clothing factors by applying separate γ -coefficients for thermal and vapor resistances in an articulated, walking manikin (16, 17, 24).

The raw data were put together in a unified spreadsheet (Microsoft Excel) for later analysis. The techniques to estimate the heat transfer equations above and all other analytical equations formulated in a previous report were also applied to this study (7, 17).

Statistical analyses. Data were analyzed using a variety of statistical modules (Statistica, version 10, Tulsa, OK and STATA, College Station, TX), the latter for testing and programming specific computerized bootstrap analyses and Monte Carlo approaches (12, 33, 34, 40, 44, 45). Simple or multiple stepwise regressions analyzed the dependence between variables. Since some subjects in night trials 1–5 were used in repeated studies, the differences between means were also analyzed using paired *t*-tests to check intraindividual sweat loss observations. For more than two tests, we used a one-way ANOVA

for repeated measures (26). Otherwise, the values were tested by unpaired *t*-tests over the various trials. The assumptions of normality and homogeneity of variance for parametric procedures were checked using Kolmogorov-Smirnov test. When the assumptions of normality or homogeneity of variance were not met, we used equivalent non-parametric tests (Kruskal-Wallis tests) for comparison of means of two independent samples (26). Following ANOVA, the data were tested using Tukey's post hoc for honestly significant differences for unpaired data or by applying a Bonferroni post hoc analysis (26).

A composite analysis was performed using pooled sweat rate data from 77 subjects completing the night marches and 550 laboratory observations from a previous study (17). The data were parsed and aggregated into a separate bootstrapping analysis to determine residual variations distinct in the original data (45). In the bootstrapping analysis, the hypothesis is that a given sample $S = \{X_1, X_2, \dots, X_n\}$ (i.e., 77 subjects from night runs) is a unique cohort of the given population $P = \{x_1, x_2, \dots, x_N\}$, where the population includes all m_{sw} data from the original PW equation analysis (12, 17). Efron (12) developed the critical statistic, $T^*_{bs} = t(S)$ that is useful in analyses of small sample bootstrapping. This statistic supersedes the classic Student's *t* to test small departures from normality. T^*_{bs} was determined as an estimate of the corresponding population parameter $\theta = t(P)$. In this analysis, θ is assumed as a vector (bold highlight) of all parameters and T^*_{bs} the corresponding vector of estimates (12, 45).

The bootstrap analogy using Efron's criterion (12) in our prediction model analysis is to derive T^*_{bs} as high as possible; if too low (<10 or so), the S (individual m_{sw} output value) is assumed to be not very well predicted by the purported equation or contributes too large an outlier of the P (or too far out of the domain of confidence limits). The bootstrap estimate of the standard error (SE) of T^*_{bs} is subsequently determined as the square root of the bootstrap variance of T^*_{bs} as specified by Efron's criteria (12).

A bootstrapped correlation matrix was next created using output predictions generated from Monte Carlo analysis applying the principles suggested by Picard (33, 34). The Monte Carlo analysis was followed by a measure of goodness of fit of the bootstrap to explain the uncertainty for the range of values of the pooled data. The goodness of fit test that was used in our study, post Monte Carlo analysis was the Schwarz-Bayesian criteria (SBC) (40), which is a function of the natural log $[\ln(n_s)]$ of the number of observations n , the sum of squared errors (SSE), and the number of independent variables $k \leq p + 1$ where k includes the intercept as shown in Eq. 10:

$$(\text{SBC}) = n \cdot \ln (\text{SSE}/n) + k \ln n \quad (10)$$

Equation 10 thus comprises the summed square of residuals $\text{SSE} = \text{Sum}_{(i=1 \text{ to } n)} [w_i (y_i - f_i)^2]$, where y_i is the observed m_{sw} data value and f_i is the predicted (PW) value from the fit; and w_i is the weighting applied to each data point, typically $w_i = 1$.

The bootstrapping analysis enabled determination of an estimated standard error (SE) of correlation of the modified PW equation (12), as noted above, using measured sweat rates in the new night field cohort data, assuming such data sets came from an anomalous multivariate population (12, 34) (i.e., uncertainty due to dissimilar field data tested vs. conventional indoor chamber data). Individual sweat rate values from the operational marches (trials 1–7) were analyzed using the data splitting technique (33). The total data set comprised all observed sweat rate values from individuals completing each trial, but trials 1–5 (Table 1, night marches) were analyzed independently from trials 6 and 7 (Table 2, transient solar marches). All data are expressed as means \pm SD or as means \pm 95% prediction intervals.

RESULTS

Night trials 1–5. Table 4 provides subject anthropometric characteristics, march distance, load, and selected physiologic responses for the seven trials. During trials 4 and 5, the calculated oxygen uptake, mean weighted skin temperature,

Table 4. Key descriptive, environmental, and physiological data from field experiments used in current validation

Trial	T _a , °C	Pw, kPa	V, m/s	Distance, km	Load, kg; L/mass, %	BSA, m ²	Body Mass, kg	T _{sk} , °C	V̇O ₂ , l/min	SR, l/h
1	25.1	2.28	0.6	24.0	30.9 ± 6.7; 40.4 ± 8.6%	1.94 ± 0.09	76.7 ± 5.5	33.81 ± 0.26	2.42 ± 0.21	1.02 ± 0.21
2	20.8	1.95	0.5	29.0	30.4 ± 7.2; 40.2 ± 10.7%	1.94 ± 0.13	77.5 ± 9.7	31.29 ± 0.41	2.43 ± 0.18	0.97 ± 0.22
3	17.4	1.30	1.3	37.0	35.2 ± 5.9; 45.8 ± 8.1%	1.94 ± 0.13	77.4 ± 9.5	29.17 ± 0.67	2.72 ± 0.30	0.72 ± 0.23
4	17.4	1.17	0.9	14.0	15.1 ± 4.5; 21.5 ± 5.1%	1.85 ± 0.10	69.9 ± 6.2	29.76 ± 0.93	1.84 ± 0.21	0.57 ± 0.16
5	20.0	1.65	1.1	14.0	17.0 ± 3.3; 24.4 ± 3.5%	1.85 ± 0.10	69.7 ± 6.3	30.91 ± 0.58	2.16 ± 0.21	0.68 ± 0.18
6	25.9	1.81	1.3	16.4	15.3 ± 4.3; 21.1 ± 6.3%	1.89 ± 0.18	73.7 ± 10.8	33.11 ± 0.33	1.69 ± 0.23	0.99 ± 0.17
7	16.2	0.94	1.4	18.3	21.0 ± 8.2; 30.8 ± 11.3%	1.83 ± 0.10	67.9 ± 6.4	29.30 ± 0.96	1.68 ± 0.22	0.61 ± 0.14

All data are means ± SD. Air temperature (T_a), ambient air movement (V), ambient water vapor pressure (Pw), distance traversed (km), load carried (L, kg), body surface area (BSA), body mass (kg), mean skin temperature (T_{sk}), and observed sweating rate (SR) are end values.

and absolute sweat loss values were lower ($P < 0.01$) compared with mean values in trials 1 and 2 (Table 4). The loads carried during trials 1, 2, and 3 were larger ($P < 0.01$) than the other trials. The load (L)/body mass (L/kg × 100) percentage carried in trials 1, 2, and 3 (ranges 40–46%, $P < 0.05$) was higher than %L/body mass apparent in the other two night trials.

Table 5 provides measured sweat rates for the night trials 1–5, the respective PW output (17), and the Shapiro (41) predicted m_{sw} values. The average deviation of each prediction output compared with measured sweat rate is provided (Δ of model – measured). For all night trials, the deviation from PW output values was not different from the measured sweat rates (mean ± SD = 28 ± 9.6 g·m⁻²·h⁻¹ for trials 1–5). For all night trials, the Shapiro (41) values deviation was greater ($P < 0.01$ to $P < 0.001$) than the measured sweat rates.

Figure 1 presents the bootstrap analysis of the PW output values (as dependent variable) plotted against measured sweat rates for trials 1–5 (77 experiments) and the previously collected laboratory data (17). The analysis employed analytic procedures using the bootstrap analysis on matched residual variances as described in METHODS (33, 45). This analysis incorporates E_{req} and E_{max} parameters implemented from PW prediction of m_{sw} . Thus the present study data served for both prediction and cross-validation of the original fitted PW equation (17, 33).

The bootstrap parameter regression of this analysis is shown in Fig. 1. The sweat rates calculated from the heat exchange variables (E_{req} and E_{max}) of trials 1–5 aggregated (closed triangles) with the PW equation vs. the sweat rates from the ARIEM lab data (open circles) had outliers that predicted lower than the 95% prediction line in 9 cases (≈1.5% of over 550 data points). Conversely, there were 12 cases of outliers predicting m_{sw} higher than 95% confidence limit (≈2% of the total data points). The higher predicted sweat rates are within the domain of variability of the bootstrapping variances inherent in the PW algorithm (12, 45) and the whole regression

equation displayed a SEE = ±69.2 g·m⁻²·h⁻¹. After 1,000 iterations, the bootstrap correlation (r_{bs}) parameter estimate defaulted to 0.81 with a standard error of the β -correlation coefficient of ±0.014 [Efron's (12) T^*_{bs} -value = 31.3, $P < 0.0001$] for the pooled data. The data now include field night run data that were combined with the original laboratory experiments. The sweat rate data exhibited essentially no heteroscedasticity (unequal variances among the groups) (26, 33, 34, 45). Following the bootstrapping analysis, a Monte Carlo parsing (34) was next executed on the combined data set to determine the optimal model selection based on an uncertainty goodness of fit of the PW equation using SBC. For the final Monte Carlo iterations, a SBC of 0.725 was derived (1 = perfect fit to the data) that suggests that the PW model using all combined data values (night + laboratory studies) still exhibits small residual random error components (0.275). As previously mentioned, a greater proportion of variance causing over- or underprediction errors is still accounted for in the lumped proportional control (β -coefficients) parameters present in the original fuzzy piecewise (PW) model (17). The data fit also conformed with the less robust Ordinary Least Squares (OLS) ($r = 0.71$, $P < 0.001$) and confirms that sweat loss prediction using the PW model was not adversely limited by any outliers changing the gain algorithm (β -coefficients) in the model prediction structure due to too high or too low sweat rates among the subjects during the various trials 1–5 (26, 33, 46). We next analyzed sweat rates in the marches where solar load was apparent.

Transient solar radiation trials 6–7. Table 4 displays the subject anthropometric characteristics, load, and selected physiologic responses for trials 6 and 7. In trial 6, 20 subjects began marching at 0330, with explicit solar gain appearing at 0500 and terminating with a maximum global solar load (gSL) of 341 W/m². During this march, T_a was 25.9°C but the effective heat stress gain owing to the increased MRT was 35.9°C. As shown in Table 2, trial 6 was a scenario that comprised two marching tasks up a mountainous gravel road (median terrain

Table 5. Measured sweat rate compared with predicted output during night marches of trials 1–5

	Trial 1	Trial 2	Trial 3	Trial 4	Trial 5
No. of subjects	13	12	12	20	20
SR, g·m ⁻² ·h ⁻¹	524 ± 96	502 ± 121	366 ± 104	307 ± 84	367 ± 96
PW prediction (Ref. 17)	493 ± 75	489 ± 55	405 ± 41	338 ± 28	393 ± 60
Shapiro prediction (Ref. 41)	854 ± 113	847 ± 106	752 ± 42	636 ± 30	727 ± 101
Δ (PW – SR)	31	13	39	31	26
Δ (Shapiro – SR)	330*	345*	386†	329*	360†

Values are means ±SD. Comparison of average deviation Δ of model output to actual sweat rate (SR): * $P < 0.01$; † $P < 0.001$; Δ (PW – SR) in all other trials, not significant.

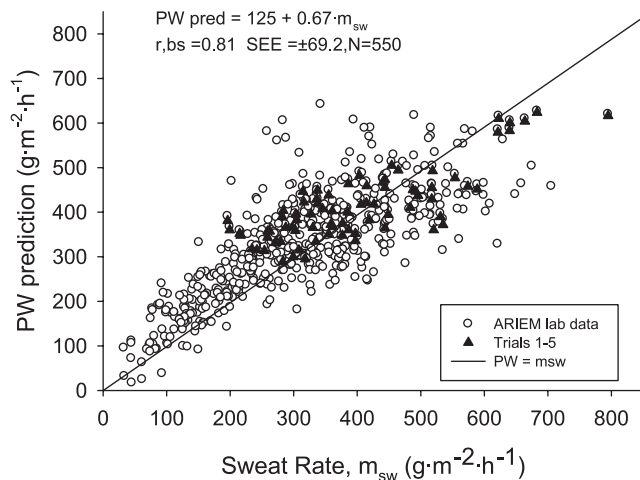


Fig. 1. PW prediction plotted as a function of sweat rate during night trials 1–5 (closed triangles) aggregated with previous laboratory results (open circles) (17). Data include bootstrapping correlation, r_{BS} (12, 34, 45); solid line is the identity line, $PW = m_{sw}$. The bootstrap estimate of standard error (SE) for the pooled data was ± 0.014 with a $T^*_b = 31$ (12). The standard error estimate of the regression (SEE) was $\pm 69.2 \text{ g}\cdot\text{m}^{-2}\cdot\text{h}^{-1}$. Typically, once the original fuzzy piecewise PW equation is applied (17, 44), this output value can be substituted in the above OLS equation ($125 + 0.67\cdot PW$) to calculate the m_{sw} required; for example, $600 \text{ g}\cdot\text{m}^{-2}\cdot\text{h}^{-1}$ determined from the equation yields $522 \text{ g}\cdot\text{m}^{-2}\cdot\text{h}^{-1} m_{sw}$, within the 95% prediction interval of the bootstrap. These data now include field night runs combined with the original lab experiments.

coefficient, $\eta = 1.3$) with work/rest cycles of 65 min work and 18 min rest followed by another march of 48 min work/15 min, and concluding with a resting period of 62 min. Total exposure time to the transient solar load was 208 min.

In trial 7, 13 subjects marched on a mixed paved and gravel road ($\eta = 1.25$). These marches began at 1420 at which time maximum global solar load (gSL) was $612 \text{ W}/\text{m}^2$. During this march, T_a was 16.2°C and the resulting MRT was 26.2°C . The work/rest marches in trial 7 continued until 1800 at which time solar load reached a nadir with minimal or no solar load. Trial 7 comprised 220 min of exposure to a transient solar load which had two separate marches with work/rest cycles that included 58 min work/15 min rest and another session that was 71 min work/14 min rest, followed by a final resting phase of 62 min.

Figure 2 shows the mean (\pm SD) solar radiation (W/m^2) as a function of time of day during the marches using R_{sol} derived from gSL for trials 6 and 7. The MRT calculated from R_{sol} and ERF increased from a value of 25.7°C to as high a 50°C during trial 6, and decreased from 58°C to as low as 16.1°C during trial 7. R_{sol} and ERF as explained in METHODS incorporated each timed output to determine E_{req} and E_{max} for later input in the modified PW prediction equation in trials 6 and 7.

Based on E_{req} and E_{max} adjustments using R_{sol} , MRT, and V_{eff} calculated for the transient solar-night trials, a revised PW (Pw_{sol}) ordinary least squares (OLS) equation for transient solar radiation conditions was developed [$m_{sw} = 0.72\cdot(Pw_{sol}) + 135$], where Pw_{sol} reflects the original PW equation (17) with E_{req} now modified to include R_{sol} ($E_{req,sol}$). The value of $E_{req,sol}$ must be first determined by pertinent solar coefficients. Table 6 provides the results of a multiple regression analysis conducted using sweat rate (dependent variable) from each of subjects completing trial 6 and 7. The output of

three prediction equations were compared: 1) Pw_{sol} as developed in the current analysis; 2) Shapiro (42), which has been discussed; and 3) HSDA, which is often used by the military to predict sweat rate for outdoor activities (3, 31). The magnitude of the β -coefficients for each prediction equation describes the relative contribution of each independent variable in the prediction of sweat rate. Table 6 indicates that Pw_{sol} had the highest β -coefficients and was the only equation that accounted for significant ($P < 0.0001$) variance contributions from each predictor variable in the orthogonal correlation structure of the multiple regression analysis (26). The Pw_{sol} output was also significantly correlated with measured sweat rates from the pooled transient solar experiments. Figure 3 also presents output showing the OLS analysis of the predictability of Pw_{sol} output values (here plotted as the independent variable) and measured m_{sw} for trials 6 and 7. A significant correlation ($r = 0.96$; $P < 0.001$) and SEE ($\pm 33.8 \text{ g}\cdot\text{m}^{-2}\cdot\text{h}^{-1}$) were detected. Once the equation is solved for the various independent variables in the heat exchange, the model output appears as a simple, practical tool in prediction of m_{sw} for a given transient solar load.

Additional data exploration. Further investigation of the combined data allowed modification of the laboratory-derived

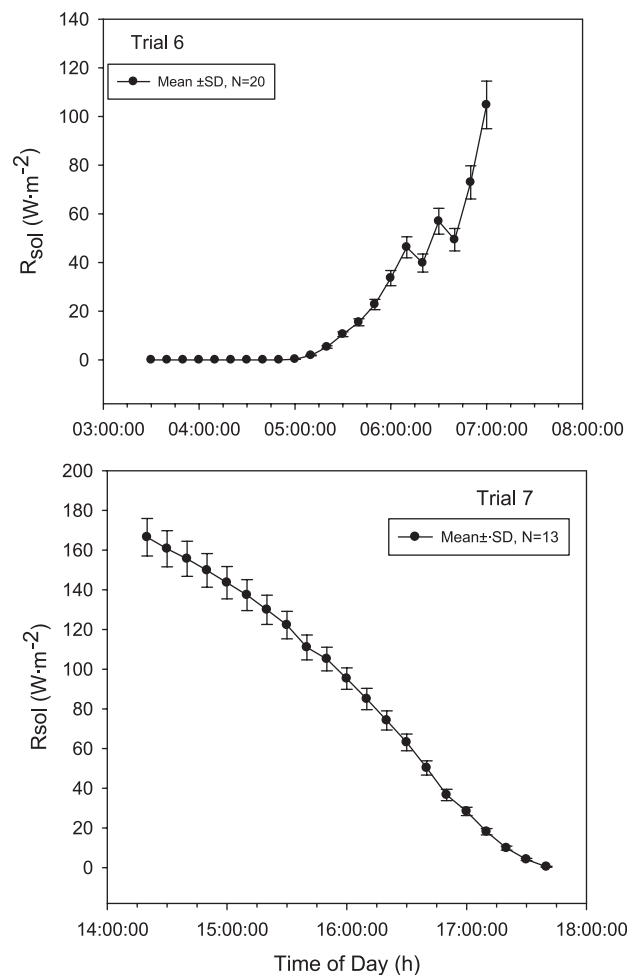


Fig. 2. R_{sol} output values (25) plotted vs. time of day during the transient solar experiments of trial 6 (top panel) and trial 7 (bottom panel). Saw-toothed dips in R_{sol} of trial 6 are due to mixed cloud formation impacting the solar flux in some trials.

Table 6. Multiple regression of sweat rate ($\text{g}\cdot\text{m}^{-2}\cdot\text{h}^{-1}$) vs. output from Shapiro equation (Ref. 42) (*Shap_out*), Heat Strain Decision Aid (Refs. 3, 31) (*HSDA*), and *PW,sol* equation for pooled data from the transient solar trials 6 and 7

Model Equation	β^*	SE of β^*	β	SE of β	$t(23)$	$P <$
HSDA	-0.020	0.062	-0.113	0.350	-0.32	0.748
<i>Pw,sol</i>	0.929	0.066	0.66	0.047	14.05	0.0001
<i>Shap_out</i> (Ref. 42)	0.066	0.075	0.21	0.240	0.87	0.391

β^* is standardized regression coefficient; β is raw regression coefficient; magnitude of β coefficients compares relative contribution of each independent variable in prediction of the sweat rate for each subject. HSDA out (Refs. 3, 31) and *Shap_out* (Ref. 42) equations were not good predictors of sweat rate ($P > 0.05$, NS) for the transient solar experiments. $N = 33$ subjects.

PW equation with a focus on cool environments during resting or low metabolic activities. Cool ($<16\text{--}18^\circ\text{C}$) ambient temperatures result in low skin wettedness, ($\omega \leq 0.15$) with water loss primarily from skin diffusion (5, 15, 19, 22). This effect takes place often when E_{max} is $\geq 400 \text{ g}\cdot\text{m}^{-2}\cdot\text{h}^{-1}$ (approximately $>270 \text{ W/m}^2$) and/or E_{req} becomes $<50 \text{ g}\cdot\text{m}^{-2}\cdot\text{h}^{-1}$ (13, 20, 22, 41). In such environments, the equation to predict sweat rates (within $131 \text{ g}\cdot\text{m}^{-2}\cdot\text{h}^{-1}$ of actual values) can now be determined from the following:

$$\text{PW, cool}(\text{g}\cdot\text{m}^{-2}\cdot\text{h}^{-1}) = 350 + 1.527 \cdot E_{\text{req}} - 0.87 \cdot E_{\text{max}} \quad (11)$$

The above equation does not alter the β -coefficients (algorithm gain) from the original *PW* equation but increases the intercept by $203 \text{ g}\cdot\text{m}^{-2}\cdot\text{h}^{-1}$ when E_{req} is low, but E_{max} is high. Therefore, for the E_{req} and E_{max} mentioned, Eq. 10 predicts $m_{\text{sw}} \sim 2.5 \text{ g/min}$ occurring with elevated wind speeds during laboratory and night (limited outdoor field) experiments.

DISCUSSION

This study validated a previously developed sweat rate prediction equation and derived pertinent biophysical-physiological corrections to modify that equation for the valid prediction of sweat rate (water needs) during transient solar radiation and cool conditions. The new *Pw,sol* and *PW,cool* equations have important implications for military and disaster relief planning and a variety of other occupational problems related to the logistical planning for water needs. We also

demonstrated that several other often used sweat prediction equations, for outside activities with a solar radiation, were far less accurate compared with the modified *Pw,sol* equation.

During the transient solar experiments, we observed high sweat rates, despite the low ambient temperatures, due to the impact of the solar gain quantified by elevated MRT. Even though load carriage and metabolic level would be considered nominal, the ambient temperatures ($T_a = 25.9^\circ\text{C}$ in *trial 6* and 16.2°C in *trial 7*) were influenced by the added rise in MRT that exacerbated the sweat rates found in *trial 6* compared with the values in *trial 7*. During the transient solar gain, average sweat rates calculated from the 20 individuals in *trial 6* were $523.4 \text{ g}\cdot\text{m}^{-2}\cdot\text{h}^{-1}$ (± 73.6 SD), compared with $332.5 \text{ g}\cdot\text{m}^{-2}\cdot\text{h}^{-1}$ (± 69.4 SD) in the 13 individuals of *trial 7* (58% increase, $P < 0.001$, nonpaired $t = 7.45$). These values amount to some 16.6 g/min higher sweat rates observed in *trial 6* vs. 10.5 g/min in *trial 7*. The necessary water requirements to sustain such sweat rates to maintain thermoregulation are greatly increased by the solar impact (ERF and MRT) during the walks despite the mild ambient conditions. Interestingly a constant cool ambient temperature (as in *trial 7*; Table 4), reducing solar radiation from a maximum (612 W/m^2) in the late afternoon to zero at night, markedly reduced sweat rates (and water needs, respectively) compared with early morning marches in which solar load gradually accumulates with a moderate air temperature. These findings are consistent with Gagge and Hardy (14) who first observed that thermoregulatory sweating (evaporative heat loss) changes were highly correlated with ERF altered by short bursts of infrared heating (heat flux from IR quartz lamps) at $T_a = 23\text{--}24^\circ\text{C}$. They also proved that as ERF increased monotonically at each higher constant ambient temperature (from 9°C to 30°C), the evaporative heat loss by sweating increased proportionately. Nielsen et al. (30) also showed similar high sweat rates during outdoor cycle exercise in the sun.

The present study confirmed our initial hypothesis that sweat rate predictive equations developed from laboratory studies (17) are suitable for matching sweat requirements (or at least were not statistically overpredictive; i.e., $\text{SEE} < \pm 70 \text{ g}\cdot\text{m}^{-2}\cdot\text{h}^{-1}$) to actual sweat loss for disparate military activities during the night time. This was an anticipated finding since the experiments involved similar conditions (T_a , RH, clothing thermal resistance values, and work rates) as in previous environmental chamber studies (7, 17). Additionally, the major finding from the present study was improvement of a sweat loss prediction equation for transient solar loads quantified by R_{sol} , ERF, and MRT. To our knowledge, this has not been possible before and may require additional investigation particularly at higher ambient (hot dry and tropical) environments.

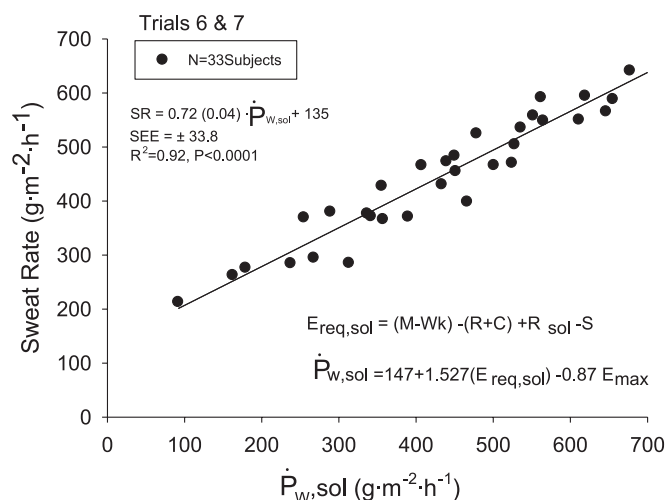


Fig. 3. Sweat rate from *trials 6* and *7* plotted as a function of *Pw,sol* equation derived from heat exchange parameters following analytical solution of $E_{\text{req,sol}}$ as explained in text.

Most experiments that involve solar load challenges in humans are done during constant thermal radiation exposures and brief time periods (14, 30). In that respect, the avenues of heat exchange (E_{req} and E_{max}) are assumed as being under steady-state conditions. Our data analysis shows that R_{sol} as a variable input into the heat balance equations can be used for estimating sweating during transient solar environments.

The prediction equations for estimating sweat rates using R_{sol} garnered from the present experiments are an important new finding because they include persistent effects of heat storage (S) as core and skin temperatures increase (37) and thereby integrate complex solar environments more rigorously than previous investigations (4, 42). We also derived by exploration of present and past (17, 41) data sets, an adjusted PW equation (PW,cool) that is applicable for cooler weather conditions when PW might predict negative sweating values because E_{req} is too low or E_{max} is too high. The adjustment requires only a change to the legacy PW equation intercept term. We recommend that these new equations should be included in current thermal models (3, 24, 46) especially for field use when solar load is present. Fundamentally, once the various discrete parameters (V_{eff} , R_{sol} , $i_{\text{m/clo}}$, etc.) influencing dynamic clothing heat transfer and walking factors are quantified into the heat balance determining E_{req} and E_{max} , the $\dot{P}w_{\text{sol}}$ equation is valid in predicting m_{sw} (within an SEE $\pm 34 \text{ g} \cdot \text{m}^{-2} \cdot \text{h}^{-1}$ or 1.1 g/min of actual sweat rate values or predicting fluid needs $\approx \pm 0.1$ liter/h) (Fig. 3). The approximation is a best case prediction scenario possible in field studies that is limited by the domain of thermal environments, metabolic intensities, and clothing ensembles studied here considering the sweat rate variability of a general population (18).

Water needs are currently estimated for the US military using HSDA or similar approaches (3, 21, 23, 28). Our past (7, 17) and this study clearly demonstrate that the PW equations provide for more accurate predictions of sweat rates during various exercise intensities and environments. A caveat of the HSDA guideline is that the input value for skin temperature executed in the calculation of dry heat loss ($R + C$) is determined by a fixed value of 36.5°C [skin saturation vapor pressure of 45 Torr (5.99 kPa)] rather than actual values as used in this study. Furthermore, the $H_{\text{s,sk}}$ values employed that determine MRT in that guideline are highly sensitive to fluctuations (γ -values) occurring in a variety of thermal and vapor resistances (20, 22, 24) as determined using thermal manikins. For example, Table 6 showed that calculation of the $H_{\text{s,sk}}$ factor in the HSDA model (3) did not predict sweat rates reliably during the transient solar trials in this study. One reason may be because $H_{\text{s,sk}}$ is a collective equation in the HSDA empirical model that incorporates MRT, but is coupled to arbitrary clothing and air movement coefficients (3). Therefore, any derived sweat loss prediction can therefore be too high or too low based on the inaccuracies of the $H_{\text{s,sk}}$ factor. A new rational multimodel also demonstrated large residuals even when applied to group data (46). The variety of equations: PW, $\dot{P}w_{\text{sol}}$, and PW,cool could be implemented in various model input interfaces (for example by using a Boolean logic “do-loop” contingency) when T_a is less than 20°C , solar load is present, wind movement is high, or cloudy outdoor activity is planned (provided all $E_{\text{req}}/E_{\text{max}}$ caveats and domain of validity are upheld).

In summary, we performed a series of outdoor military field studies in which sweat rate was quantified in 110 soldiers exercising during night trials and during transient solar radiation conditions. We validated our recently published sweat rate prediction equation (17) for outdoor military activities and modified it so it predicts m_{sw} accurately for transient solar radiation and cooler ambient conditions. We compared our PW sweat prediction equations to other existing predictions equations and established that PW was an improved calculation readily applicable during field training exercises with ($\dot{P}w_{\text{sol}}$), without (original PW) transient solar loads, and finally when environmental conditions embrace low E_{req} and high E_{max} capacities (PW,cool) during moderate exercise intensities. The family of PW sweat prediction equations allows easy implementation tools in civilian, sports, and military medicine communities needed to estimate water needs during a variety of heat stress/exercise conditions.

ACKNOWLEDGMENTS

We appreciate the efforts of the volunteer subjects and the technical staff of the Heller Institute, Sheba Medical Center, Israel during these experiments and thank them for their participation in the various experimental protocols. We thank Dr. Rick Picard, Los Alamos National Laboratory, Los Alamos, NM, for access to his cross-validation papers and salient information regarding Monte Carlo ex post facto sampling.

The opinions or assertions contained herein are the private views of the authors and should not be construed as official or reflecting the views of the Army or the Department of Defense and/or the New Mexico State University Regents. Approved for public release: Distribution unlimited.

GRANTS

This study was funded by research contracts from the U.S. Army Medical Research and Materiel Command.

DISCLOSURES

No conflicts of interest, financial or otherwise, are declared by the author(s).

AUTHOR CONTRIBUTIONS

Author contributions: R.R.G., S.N.C., D.S.M., A.H., and M.N.S. conception and design of research; R.R.G., B.R.E., D.S.M., A.H., T.L.E., and M.N.S. analyzed data; R.R.G., S.N.C., B.R.E., D.S.M., A.H., T.L.E., and M.N.S. interpreted results of experiments; R.R.G. prepared figures; R.R.G., S.N.C., and M.N.S. drafted manuscript; R.R.G., S.N.C., B.R.E., D.S.M., A.H., T.L.E., and M.N.S. edited and revised manuscript; R.R.G., S.N.C., B.R.E., D.S.M., A.H., T.L.E., and M.N.S. approved final version of manuscript; S.N.C., B.R.E., D.S.M., A.H., and T.L.E. performed experiments.

REFERENCES

1. American Society of Heating, Refrigerating, and Air-Conditioning Engineers. *Fundamentals Handbook: Physiological Principles, Comfort, Health*. Atlanta, GA: ASHRAE, 1993, chapt. 8.
2. Arens E, Gonzalez RR, Berglund LG. Thermal comfort under an extended range of environmental conditions. *ASHRAE Trans*. V92. PA.1, 1986.
3. Blanchard LA, Santee WR. *Comparison of USARIEM Heat Strain Decision Aid, Mobile Heat Stress Monitor, and Existing Army Guidelines for Warm Weather Training* (Technical Report T08/07). Natick, MA: U.S. Army Research Institute of Environmental Medicine, 2008.
4. Breckenridge JR, Goldman RF. Solar heat load in man. *J Appl Physiol* 31:659–663, 1971.
5. Candas V, Libert JP, Vogt JJ. Human skin wettedness and evaporative efficiency of sweating. *J Appl Physiol* 46: 522–528, 1979.
6. Carter R, Chevront SN, Montain SJ, Sawka MN. *Prediction and Validation of Warfighter Fluid Requirements*. NATO Research and Technology Organization HFM-086 Symposium on “Maintaining Hydration: Issues, Guidelines, and Delivery.” Boston, MA, December 10–11, 2003 (available at www.rta.nato.int).

7. **Cheuvront SN, Montain SJ, Goodman DA, Blanchard L, Sawka MN.** Evaluation of the limits to accurate sweat loss prediction during prolonged exercise. *Eur J Appl Physiol* 101: 215–224, 2007.
8. **Departments of the Army and Air Force.** *Heat Stress Control and Heat Casualty Management.* TBMED 507/UFPAM 48–152(I). Washington, DC: Government Printing Office, 2003.
9. **Department of Defense.** Directive 4705.1. *Management of Land-Based Water Resources in Support of Contingency Operations.* 1992.
10. **Directorate of Combat Developments.** *Water Consumption Planning Factors.* Ft. Lee, VA: U.S. Army CASCOM, 1999.
11. **Dupont FJ, Dean C.** *Hydration and the Modern Warrior's Load.* NATO Research and Technology Organization HFM-086 Symposium on "Maintaining Hydration: Issues, Guidelines, and Delivery." Boston, MA, December 10–11, 2003 (available at www.rta.nato.int).
12. **Efron B.** *Jackknife After Bootstrap Standard Errors and Influence Factors.* (Technical Report No. 134). Stanford, CA: Division of Biostatistics, Stanford University, 1990.
13. **Fanger PO.** *Thermal Comfort: Analysis and Applications in Environmental Engineering.* New York: McGraw-Hill Book, 1972.
14. **Gagge AP, Hardy JD.** Thermal radiation exchange of the human by partitioned calorimetry. *J Appl Physiol* 23: 248–258, 1967.
15. **Gagge AP, Gonzalez RR.** Mechanisms of heat exchange: biophysics and physiology. In: *Handbook of Physiology: Environmental Physiology.* Bethesda, MD: Am. Physiol. Soc., 1996, p. 45–84.
16. **Gonzalez RR.** Infrared radiation and human thermal comfort. In: *Micro-waves and Thermoregulation,* edited by Adair ER. New York: Academic, 1983, p. 109–137.
17. **Gonzalez RR, Cheuvront SN, Montain SJ, Goodman DA, Blanchard LA, Berglund LG, Sawka MN.** Expanded prediction equations of human sweat loss and water needs. *J Appl Physiol* 107: 379–388, 2009.
18. **Greenleaf JE, Averkin EG, Sargent F.** Water consumption by man in a warm environment: a statistical analysis. *J Appl Physiol* 21: 93–98, 1966.
19. **Havenith G.** Individualized model of human thermoregulation for the simulation of heat stress response. *J Appl Physiol* 90: 1943–1954, 2001.
20. **Havenith G, Richards MB, Wang X, Brode P, Candas V, den Hartog E, Holmer I, Kuklane K, Meinander H, Nocker W.** Apparent latent heat of evaporation from clothing: attenuation and "heat pipe" effects. *J Appl Physiol* 104: 142–149, 2008.
21. **Institute of Medicine.** *Dietary Reference Intakes for Water, Potassium, Sodium, Chloride, and Sulfate.* Washington, DC: The National Academies Press, 2005.
22. **Kakitsuba N, Gaul K, Michna H, Mekjavic IB.** Dynamic moisture permeation through clothing. *Aviat Space Environ Med* 59: 49–53, 1988.
23. **Kolka MA, Latzka WA, Montain SJ, Corr WP, O'Brien KK, Sawka MN.** Effectiveness of revised fluid replacement guidelines for military training in hot weather. *Aviat Space Environ Med* 74: 242–246, 2003.
24. **Kraning KK, Gonzalez RR.** A mechanistic computer simulation of human work in heat that accounts for physical and physiological effects of clothing, aerobic fitness, and progressive dehydration. *J Therm Biol* 22: 331–342, 1997.
25. **Matthew WT, Santee WR, Berglund LG.** *Solar Load Inputs for USARIEM Thermal Strain Models and the Solar Radiation-Sensitive Components of the WBGT Index* (Technical Report T01/13–01). Natick, MA: U.S. Army Research Institute of Environmental Medicine, 2001.
26. **Miller RG.** *Simultaneous Statistical Inference* (2nd ed.). New York: Springer, 1981.
27. **Mitchell D, Wyndham CH.** Comparison of weighting formulas for calculating mean skin temperature. *J Appl Physiol* 26: 616–622, 1969.
28. **Montain SJ, Latzka WA, Sawka MN.** Fluid replacement recommendations for training in hot weather. *Mil Med* 164: 502–508, 1999.
29. **Montain SJ, Cheuvront SN, Sawka MN.** Exercise-associated hyponatremia: quantitative analyses for understanding etiology and prevention. *Br J Sports Med* 40: 98–106, 2006.
30. **Nielsen B, Kassow K, Aschengreen FE.** Heat balance during exercise in the sun. *Eur J Appl Physiol* 58: 189–196, 1988.
31. **Pandolf KB, Stroschein LA, Drolet LL, Gonzalez RR, Sawka MN.** Prediction modeling of physiological responses and human performance in the heat. *Comput Biol Med* 16: 319–329, 1986.
32. **Pandolf KB, Givoni B, Goldman RF.** Predicting energy expenditure with loads while standing or walking very slowly. *J Appl Physiol* 43: 577–581, 1977.
33. **Picard RR, Cook RD.** Cross-validation of regression models. *J Am Stat Assoc* 79: 575–583, 1984.
34. **Picard RR, Booth TE.** Ensuring finite moments in Monte Carlo simulations via iterated ex post facto sampling. *Math Comp Simul* 79: 2106–2121, 2009.
35. **Santee WR, Blanchard LA, Speckman KL.** *Load Carriage Development and Testing with Field Data* (Technical Note TN03–3). Natick, MA: U.S. Army Research Institute of Environmental Medicine, 2003.
36. **Sawka MN.** Body fluid responses and hypohydration during exercise-heat stress. In: *Human Performance Physiology and Medicine at Terrestrial Extremes,* edited by Pandolf, KB, Sawka, MN, Gonzalez, RR. Traverse City, MI: Cooper Publishing Group, 1988, p. 227–266.
37. **Sawka MN, Wenger CB.** Physiological responses to acute exercise-heat stress. In: *Human Performance Physiology and Medicine at Terrestrial Extremes,* edited by Pandolf, KB, Sawka, MN, Gonzalez, RR. Traverse City, MI: Cooper Publishing Group, 1988, p. 97–151, 1988.
38. **Sawka MN, Cheuvront SN, Carter R.** Human water needs. *Nutr Rev* 63: S30–S39, 2005.
39. **Sawka MN, Eichner ER, Maughn RJ, Montain SJ, Stachenfeld N.** ACSM position stand: exercise and fluid replacement. *Med Sci Sports Exerc* 39: 377–390, 2007.
40. **Schwarz G.** Estimating the dimension of a model. *Ann Statistics* 6: 461–464, 1978.
41. **Shapiro Y, Pandolf KB, Goldman RF.** Predicting sweat loss response to exercise, environment and clothing. *Eur J Appl Physiol* 48: 83–96, 1982.
42. **Shapiro Y, Moran D, Epstein Y, Stroschein L, Pandolf KB.** Validation and adjustment of the mathematical prediction model for human sweat rate responses to outdoor environmental conditions. *Ergonomics* 38: 981–986, 1995.
43. **Shibasaki M, Kondo N, Crandall CG.** Non-thermoregulatory modulation of sweating in humans. *Exerc Sport Sci Rev* 31: 34–39, 2003.
44. **Tseng YT, Durbin P, Tseng GH.** Using fuzzy piecewise regression analysis to predict non-linear time series of turbulent flows with automatic change-point detection. *Flow Turbul Combust* 67: 81–106, 2001.
45. **Uraibi HS, Midi H, Talib BA, Youusif J.** Linear regression model selection based on robust bootstrapping technique. *Am J Appl Sciences* 6: 1191–1198, 2009.
46. **Xu X, Santee WR.** Sweat loss prediction using a multi-model approach. *Int J Biometeorol* 55: 501–508, 2011.